Geosci. Model Dev. Discuss., doi:10.5194/gmd-2016-21, 2016
Manuscript under review for journal Geosci. Model Dev.
Published: 11 February 2016
© Author(s) 2016. CC-BY 3.0 License.

Geoscientific Model Development Discussions

Implementation of state-of-the-art ternary new particle formation scheme to the regional chemical transport model PMCAMx-UF in Europe

Elham Baranizadeh[1], Benjamin N. Murphy[2,3], Jan Julin[1,2], Saeed Falahat[2,4], Carly L. Reddington[5], Antti Arola[6], Santtu Mikkonen[1], Christos Fountoukis[7], David Patoulias[8], Andreas Minikin[9], Thomas Hamburger[10], Ari Laaksonen[1,11], Spyros N. Pandis[8,12,13], Hanna Vehkamäki[14], Kari E. J. Lehtinen[1,6], Ilona Riipinen[2]

[1]Department of Applied Physics, University of Eastern Finland, Kuopio, Finland
[2]Department of Environmental Science and Analytical Chemistry (ACES), Stockholm University, Stockholm, Sweden
[3]Now at the National Exposure Research Laboratory, US Environmental Protection Agency, Research Triangle Park, USA
[4]Now at the Swedish Meteorological and Hydrological institute (SMHI), Norrköping, Sweden
[5]Institute for Climate and Atmospheric Science, School of Earth and Environment, University of Leeds, Leeds, UK
[6]Finnish Meteorological Institute, Kuopio, Finland
[7]Qatar Environment and Energy Research Institute (QEERI), Hamad Bin Khalifa University (HBKU), Qatar Foundation, Doha, Qatar
[8]Department of Chemical Engineering, University of Patras, Patras, Greece
[9]German Aerospace Agency DLR, Oberpfaffenhofen, Germany
[10]Norwegian Institute for Air Research (NILU), Oslo, Norway
[11]Climate research Unit, Finnish Meteorological Institute, Helsinki, Finland
[12]Institute of Chemical Engineering Sciences, Foundation for Research and Technology Hellas (ICEHT/FORTH), Patras, Greece
[13]Department of Chemical Engineering, Carnegie Mellon University, Pittsburgh, PA, USA
[14]Division of Atmospheric Sciences, Department of Physics, University of Helsinki, Helsinki, Finland

Abstract

The particle formation scheme within PMCAMx-UF, a three dimensional chemical transport model, was updated with particle formation rates for the ternary H_2SO_4-NH_3-H_2O pathway simulated by the Atmospheric Cluster Dynamics Code (ACDC) using quantum chemical input data. The model was applied over Europe for May 2008, during which the EUCAARI-LONGREX campaign was carried out providing aircraft vertical profiles of aerosol number concentrations. The updated model reproduces the observed number concentrations of particles larger than 4 nm within one order of magnitude throughout the atmospheric column. This reasonable agreement is very encouraging considering the fact that no

Geosci. Model Dev. Discuss., doi:10.5194/gmd-2016-21, 2016
Manuscript under review for journal Geosci. Model Dev.
Published: 11 February 2016
© Author(s) 2016. CC-BY 3.0 License.

Geoscientific Model Development Discussions

semi-empirical fitting was needed to obtain realistic particle formation rates. The cloud adjustment scheme for modifying the photolysis rate profiles within PMCAMx-UF was also updated with the TUV (Tropospheric Ultraviolet and Visible) radiative transfer model. Results show that although the effect of the new cloud adjustment scheme on total number concentrations is small, enhanced new particle formation is predicted near cloudy regions. This is due to the enhanced radiation above and in the vicinity of the clouds, which in turn leads to higher production of sulfuric acid. The sensitivity of the results to including emissions from natural sources is also discussed.

1 Introduction

Formation of new particles from atmospheric vapors (new particle formation, NPF) is potentially an important source of particulate matter in the atmosphere, especially in the ultrafine (<100 nm in diameter) size range (Kulmala et al., 2004; Merikanto et al., 2009; Jung et al., 2010; Fountoukis et al., 2012; Kerminen et al., 2012; Fuzzi et al, 2015). In the past, in modeling studies on the role of in-situ NPF as a particle source, particle formation has been represented with various parameterizations including binary (Vehkamäki et al., 2002) or ternary (Napari et al., 2002) nucleation based on the classical nucleation theory (CNT), semi-empirical activation (Kulmala et al., 2006), kinetic (McMurry, 1980) or organic-enhanced (Paasonen et al., 2010) NPF and/or ion mediated nucleation (Yu and Luo, 2009). These parameterizations have generally assumed sulfuric acid (H_2SO_4), water (H_2O), ammonia (NH_3), or different organic species as the compounds forming the new particles. The activation, kinetic and organic-enhanced mechanisms are semi-empirical, based on the observed dependence of particle formation rates on concentrations of sulfuric acid and/or organic vapors (Sihto et al., 2006; Paasonen et al., 2010). The advantage of such methods is that they are simple and produce nucleation rates of the same order as those observed. However, as they are fit to specific experiments usually at ground level, they are most reliable at locations and conditions similar to those at which the data has been obtained. The ternary H_2SO_4-H_2O-NH_3 parameterization by Napari et al. (2002) has been used with some success (Adams and Seinfeld, 2002; Jung et al., 2008; Jung et al., 2010; Fountoukis et al., 2012; Westervelt et al., 2014), but with quite drastic correction factors necessary to reproduce ambient particle number concentrations. In many previous studies (Spracklen et al., 2006; Makkonen et al., 2009; Yu et al., 2010) the binary H_2SO_4-H_2O nucleation has been assumed to dominate in the upper atmosphere and be negligible at lower altitudes, and it has often been superimposed with one of the other mechanisms.

Sulfuric acid, water and ammonia have long been established as important molecules forming new particles in the atmosphere (Korhonen et al., 1999; Kulmala et al., 2000; Laaksonen et al., 2008). However, standard theoretical descriptions of the ternary H_2SO_4-H_2O-NH_3 particle formation pathway have not been able to reproduce measured particle formation rates – hence the need to resort to semi-empirical parameterizations and correction factors to describe this process in atmospheric models.

Geosci. Model Dev. Discuss., doi:10.5194/gmd-2016-21, 2016
Manuscript under review for journal Geosci. Model Dev.
Published: 11 February 2016
© Author(s) 2016. CC-BY 3.0 License.

Recent experimental (Kirkby et al., 2011; Almeida et al., 2013; Jen et al., 2014) and computational developments have, however, changed this picture drastically. Flexible computational models (such as the Atmospheric Cluster Dynamics Code, ACDC, Olenius et al., 2013) which simulate the kinetics of a population of molecular clusters combined with cluster free energies calculated from first-principles methods, can now reproduce laboratory observations of particle formation rates in H_2SO_4-NH_3 as well as H_2SO_4-amine systems with reasonable accuracy (Almeida et al., 2013), without the need for empirical scaling of the predicted particle formation rate.

Predictions of particle number concentration from regional-scale chemical transport models have been evaluated typically with data from ground-level observations (Jung et al., 2008; Matsui et al., 2011a, 2013c; Fountoukis et al., 2012; Cui et al., 2014; Lupascu et al., 2015). Meanwhile, there is much to gain from assessing the model against vertically-resolved particle number observations, as many of the uncertainties in the model relate to particle scavenging, by hydrometeors as well as other particles, and mixing of air masses. The possible biases introduced from parameterizing new particle formation rates with ground-level data makes it all the more imperative to evaluate and constrain models with observations taken at altitude. Recent studies (Reddington et al., 2011; Lupascu et al., 2015) have begun assessing global- and regional-scale models in this way against data from European and US field campaigns involving aircraft measurements. Furthermore, it is worthwhile to explore the vertical variability in chemical and environmental precursors to NPF (e.g. H_2SO_4, NH_3, *T*, RH, etc.) and particle number concentrations.

In this work we describe the implementation of a H_2SO_4-H_2O-NH_3 new particle formation scheme based on the output of the ACDC model to the regional chemical transport model PMCAMx-UF (Jung et al., 2010, Fountoukis et al., 2012). We test the new scheme by simulating the evolution of atmospheric gas-phase and aerosol particle concentrations during May 2008 in Europe. We evaluate the model against ground-based and airborne observations of aerosol particle number size distributions during the simulated period. Furthermore, we implement an updated radiative transfer scheme TUV (Tropospheric Ultraviolet and Visible radiative transfer model; Madronich, 2002) for PMCAMx-UF and discuss its implications for predictions of NPF and particle number concentrations in the European domain.

2 Methods

2.1 PMCAMx-UF model description

PMCAMx-UF is a three-dimensional regional chemical transport model that simulates both the size-dependent particle number and chemically-resolved mass concentrations (Jung et al. 2010). PMCAMx-UF utilizes the framework of the air quality model PMCAMx (Gaydos et al., 2007, Karydis et al., 2007),

Geosci. Model Dev. Discuss., doi:10.5194/gmd-2016-21, 2016
Manuscript under review for journal Geosci. Model Dev.
Published: 11 February 2016
© Author(s) 2016. CC-BY 3.0 License.

Geoscientific Model Development Discussions

where the description of vertical and horizontal advection and dispersion, wet and dry deposition, and gas-phase chemistry are based on the CAMx air quality model, and the variable size-resolution model of Fahey and Pandis (2001) is used for aqueous-phase chemistry. To treat the aerosol microphysics, including NPF, condensation and coagulation, PMCAMx-UF uses the Dynamic Model for Aerosol Nucleation (DMAN) module by Jung et al. (2006). DMAN uses the Two-Moment Aerosol Sectional (TOMAS) algorithm (Adams and Seinfeld, 2002) to track the aerosol number and mass distributions. DMAN divides the aerosol particles into 41 logarithmically-spaced size bins between 0.8 nm and 10 μm.

The aerosol species modeled in PMCAMx-UF include sulfate, ammonium, water, elemental carbon, crustal material, chloride, sodium, nitrate, primary organic aerosol and four secondary organic aerosol surrogate compounds. The version of TOMAS used in the model applied here tracks explicitly the mass transfer of sulfate and ammonium while that of water is treated assuming equilibrium. Within the DMAN aerosol microphysics module the remaining compounds are represented by inert surrogate species. The pseudo-steady-state approximation method (Pierce and Adams, 2009), which assumes steady-state concentration for sulfuric acid, is used for the calculation of NPF and sulfuric acid condensation rates. The condensation of ammonia is calculated independently following the approach described in Jung et al. (2006).

New particle formation rates in the standard version of PMCAMx-UF have been calculated in previous studies using a scaled version of the ternary H_2SO_4-NH_3-H_2O parametrization by Napari et al. (2002), hereafter referred to as the "scaled" Napari parameterization. The original Napari parameterization is based on predictions of the CNT assuming that the energetics of the molecular clusters follow bulk thermodynamics. While it has been shown to perform better than a range of other nucleation parameterizations in predicting the occurrence of new particle formation events (Jung et al. 2008), it is also known to overpredict ultrafine particle number concentrations (Gaydos et al., 2005; Yu et al., 2006a; Jung et al., 2006; Merikanto et al., 2007b; Zhang et al., 2010). Thus a semi-empirical correction factor of 10^{-6} has been applied previously in PMCAMx-UF to scale the formation rates produced by the Napari parameterization and better match the observations (Jung et al., 2010; Fountoukis et al., 2012; Ahlm et al., 2013).

Encouraged by the good agreement between particle formation rates predicted by the ACDC model and the state-of-the-art experimental data (Almeida et al., 2013), we have updated the particle formation scheme within PMCAMx-UF with ACDC-based particle formation rates for the NH_3-H_2SO_4-H_2O (see Sect. 2.2 for details and the Results section for comparison to the scaled Napari parameterization). In addition to applying the ternary H_2SO_4-NH_3- H_2O NPF scheme, we also include a binary H_2SO_4-H_2O

Geosci. Model Dev. Discuss., doi:10.5194/gmd-2016-21, 2016
Manuscript under review for journal Geosci. Model Dev.
Published: 11 February 2016
© Author(s) 2016. CC-BY 3.0 License.

NPF pathway. This pathway is operating simultaneously with the ternary pathway and is based on the Vehkamäki et al. (2002) CNT-parameterization.

PMCAMx-UF was applied for the period of May 2008 for the European domain which consists of a 5400 × 5832 km^2 region with a 36 × 36 km^2 grid resolution and 14 vertical layers reaching an altitude of approximately 20 km. The PMCAMx-UF output data are hourly averaged. The meteorological inputs, described in detail in Fountoukis et al. (2011; 2012), were created using the Weather Research and Forecasting model version 2 (Skamarock et al., 2005) and include horizontal wind components, vertical dispersion coefficients, temperature, pressure, water vapor mixing ratios, cloud optical depths and rainfall rates. Hourly gridded emissions include anthropogenic emission rates of primary particulate matter and gases. For the particle emissions the Pan-European anthropogenic Particle Number Emission Inventory (Denier van der Gon et al., 2009; Kulmala et al., 2011) and the Pan-European Carbonaceous Aerosol Inventory (Kulmala et al., 2011) were used. The anthropogenic gas emissions include both land emissions from the GEMS data set (Visschedijk et al., 2007) and international shipping emissions. These emission inputs are the same as have been used previously for the May 2008 period in PMCAMx-UF (in Fountoukis et al., 2012; Ahlm et al., 2013), and thus in order to enable comparison to the previous works these inputs are used in all of the base model runs of the present paper. To assess how much the particle number concentrations are affected by emissions from natural sources we have performed simulations with and without these emissions. The natural emissions include both particulate matter and gases and combine three different datasets: emissions from ecosystems based on the MEGAN model (Guenther et al., 2006), marine emissions based on the model of O'Dowd et al. (2008), and wildfire emissions (Sofiev et al., 2008a, b).

2.2 Improved treatment of the ternary NPF pathway

The ternary H_2SO_4–NH_3–H_2O particle formation rate at approximately 1.2 nm in mass diameter was calculated with the Atmospheric Cluster Dynamics Code (ACDC; Olenius et al., 2013; Almeida et al., 2013; Henschel et al., 2015). ACDC simulates the dynamics of a population of molecular clusters by numerically solving the cluster birth–death equations. Instead of considering only collisions and evaporations of single vapor molecules, an often-used assumption applied in the CNT framework, ACDC allows all possible collision and fragmentation processes within the cluster population. As input the code needs the corresponding rate constants, of which the most challenging to assess are the cluster evaporation rates, generally calculated from the free energies of formation of the clusters. The evaporation rates play a significant role in determining the number concentration and consequently the formation rate of small particles. The liquid drop model, commonly used in CNT to calculate the free energies of cluster formation, is based on macroscopic thermodynamics and is thus not expected to give reliable results for small clusters (Merikanto et al., 2007a). The most accurate theoretical method to

Geosci. Model Dev. Discuss., doi:10.5194/gmd-2016-21, 2016
Manuscript under review for journal Geosci. Model Dev.
Published: 11 February 2016
© Author(s) 2016. CC-BY 3.0 License.

compute the free energies of clusters consisting of specific molecules is quantum chemistry. This modeling approach is able to reproduce the general trends in cluster formation, and leads to, thus far, the best quantitative agreement between observations and modeling with no fitting parameters (Almeida et al., 2013).

In the ACDC simulations of this work, hard-sphere collision rates were used for the collision rate coefficients, and the evaporation rate coefficients were calculated from the Gibbs free energies of formation of the clusters computed with quantum chemical methods at the B3LYP/CBSB7//RICC2/aug-cc-pV(T+d)Z level (Ortega et al., 2012; Henschel et al., 2014). This level of theory has been tested against higher level methods and was shown to give reliable cluster formation free energies at an affordable computational cost. The simulation included clusters containing up to three H_2SO_4 and three NH_3 molecules, hydrated by up to four or five water molecules. Sulfuric acid and ammonia were explicitly treated in the simulation, and water was implicitly included by assuming that the clusters are in equilibrium with respect to water and by using hydrate averaged collision and evaporation rates. An external sink term corresponding to scavenging by larger particles was used for all the clusters. The steady-state particle formation rate was obtained as the flux of clusters growing out of the simulation system considering boundary conditions based on cluster stability. Details of the simulated ternary H_2SO_4–NH_3–H_2O system can be found in Henschel et al. (2015).

The ACDC results were implemented in the PMCAMx-UF framework as a look-up table consisting of a comprehensive set of particle formation rates computed at different values of H_2SO_4 and NH_3 concentrations, temperature, RH, and coagulational loss rate due to scavenging by the population of larger particles (described by the condensation sink, see e.g. Dal Maso et al., 2002). The formation rate data produced by theoretical models have been traditionally fitted to a multivariable functional form (Napari et al, 2002; Merikanto et al., 2007b), with the resulting parameterization then utilized by large scale models. However, finding a suitable functional form to cover satisfactorily the whole parameter space becomes increasingly difficult with increasing number of input parameters, with increasing number of species participating in NPF, and with the tendency of formation rates to exhibit rapid, step function–like changes with respect to one or more parameters. Thus interpolating from a look-up table provides formation rates that are more closely in line with the original theoretical model, with a relatively minor additional computational cost. The parameter space encompasses sulfuric acid concentration between $1.00 \cdot 10^4$ and $3.16 \cdot 10^9$ molecules cm^{-3}, ammonia concentration between 10^6 and 10^{11} molecules cm^{-3}, relative humidity between 0 and 100 %, temperature between 180 and 320 K and condensation sink between 10^{-5} and 10^{-1} s^{-1}. These conditions bound the environmental and chemical conditions predicted by typical PMCAMx-UF runs for Europe in May. PMCAMx-UF uses multilinear interpolation to extract formation rates from the look-up table. The newly-formed particles added to PMCAMx-UF are assumed to have a diameter of 1.2 nm, corresponding to the size for which the ACDC

Geosci. Model Dev. Discuss., doi:10.5194/gmd-2016-21, 2016
Manuscript under review for journal Geosci. Model Dev.
Published: 11 February 2016
© Author(s) 2016. CC-BY 3.0 License.

formation rates were calculated. This approach provides PMCAMx-UF with formation rates that are based on the full kinetic treatment of the cluster population.

2.3 Radiative transfer and photolysis rates

Aerosols and clouds can enhance or reduce photolysis of relevant gas-phase chemical species in the atmosphere by reflecting, scattering, or absorbing solar radiation. Modifications of photolysis rates via this interaction lead to changes in the production rate of sulfuric acid, which lead directly to changes in the new particle formation rates. Previous versions of PMCAMx-UF employed a parameterization originally used by the Regional Acid Deposition Model (RADM; Chang et al., 1987) to treat the modification of photolysis rates due to cloud presence. This approach required the cloud optical depth from the meteorological input data and the solar zenith angle in order to calculate the time- and layer-dependent adjustment factors for the photolysis rates. This method, however, did not use aerosol concentrations predicted online by the transport model. Instead, a reference aerosol profile was used for every time step and column of grid cells.

To more realistically treat the effects of clouds on the photolysis rates profile of the atmospheric column, we updated the online approach in PMCAMx-UF to a streamlined form of the two-stream radiative transfer module, TUV (Tropospheric Ultraviolet and Visible radiative transfer model; Madronich, 2002). The implementation of TUV was completed as documented by Emery et al. (2010). This simplified module employs a reduced number of wavelength bands and plane-parallel two-stream approximations. Inputs needed include the cloud optical depth, solar zenith angle, three-dimensional aerosol concentration profile, and optical properties of the aerosol components provided by Takemura et al., 2002.

The total cloud optical depth τ above a current grid cell up to the top of troposphere is here approximated by

$$\tau = \frac{3L\Delta z_c}{2\rho_w r}, \quad (1)$$

where L is the mean cloud liquid water (g m^{-3}) , Δz_c is the mean depth of cloudy layer (m) in the cell, ρ is the density of water (10^6 g m^{-3}), and r is the mean cloud drop radius (10^{-5} m). The grid cells with cloud optical depth less than 5 are considered as optically thin clouds (or cloud-free conditions), so that the TUV module is not called for such grid cells. The module also takes as input the time- and space-dependent vertical profile of dry and wet (with an RH-dependent lensing effect) aerosols predicted by PMCAMx-UF.

Geosci. Model Dev. Discuss., doi:10.5194/gmd-2016-21, 2016
Manuscript under review for journal Geosci. Model Dev.
Published: 11 February 2016
© Author(s) 2016. CC-BY 3.0 License.

Geoscientific Model Development Discussions

The module outputs a modified actinic flux that can then be applied, using the clear-sky actinic flux for reference, to adjust the clear-sky photolysis rates. Adjustments due to clouds and aerosols tend to reduce photolysis below clouds but often enhance rates above clouds because of the reflection from the top of the cloud. Emery et al. (2010) implemented the module in the Comprehensive Air Quality Model with Extensions (CAMx) and evaluated it for ozone prediction in the Houston area. That study found decreased ozone surface concentrations with maximum decreases of approximately 10 ppb. However, they did not report the impacts that the radiation feedback would have on particulate mass or number. We compare particle number and sulfuric acid vapor profiles with and without the radiation update in place to better understand the importance of correctly representing this phenomenon.

2.4 Model evaluation with particle number and size distribution data

During the European Aerosol Cloud Climate and Air Quality Interactions (EUCAARI) project (Kulmala et al., 2009; 2011) particle number size distributions within the atmospheric boundary layer were measured at various European Supersites for Atmospheric Aerosol Research (EUSAAR). May 2008 was one of the intensive observation periods of the project. In this study the predicted ground-level hourly-averaged particle number concentrations are evaluated against the data from Aspvreten (Sweden), Cabauw (Netherlands), Hyytiälä (Finland), Ispra (Italy), Mace Head (Ireland), Melpitz (Germany) and Vavihill (Sweden) similarly to Fountoukis et al. (2012). These locations represent seven different types of European environments (Ahlm et al., 2013). More information about the characteristics and topography of these sites is available elsewhere (Asmi et al., 2011 and Fountoukis et al., 2012). The particle size distribution measurements were carried out using either a Differential Mobility Particle Sizer (DMPS) or Scanning Mobility Particle Sizer (SMPS) systems in the mobility diameter size range above 10 nm.

To evaluate the vertical profile of the particle size distribution, we used the observational data measured by the German DLR Falcon 20 and the British FAAM BAe-146 research aircrafts, operating between 6 and 24 May 2008. The aircraft data was collected during the LONGREX campaign (Hamburger et al., 2011), which was also a part of the EUCAARI project. The FAAM BAe-146 flights mainly flew in the boundary layer and lower free troposphere while the DLR Falcon 20 aircraft mostly probed the free troposphere up to the tropopause level (Hamburger et al., 2011). The Condensation Particle Size Analyser (CPSA) (Fiebig et al., 2005; Feldpausch et al., 2006), installed aboard the DLR Falcon 20, and the Passive Cavity Aerosol Spectrometer Probe (PCASP-100X) (Liu et al., 1992), operated aboard both aircraft, measured the particle number concentrations. Consistent with Reddington et al. (2011), we used the measurements from two channels of the CPSA onboard the DLR Falcon 20 with lower cut-off diameters of 4 and 10 nm, yielding the number concentrations of particles above these sizes, denoted as N_4 and N_{10}. The temporal resolution of the CPSA dataset is 1 s. The nominal size range of PCASP-100X is 0.12-3.5 µm with 15 channels. The PCASP-100X raw data was sampled with 1 Hz frequency, but the

Geosci. Model Dev. Discuss., doi:10.5194/gmd-2016-21, 2016
Manuscript under review for journal Geosci. Model Dev.
Published: 11 February 2016
© Author(s) 2016. CC-BY 3.0 License.

data used here is based on averaging over a constant interval of 5 s. We used the measured particle number concentrations obtained from channels 3 to 10 of the PCASP-100X covering the diameter range of 160-1040 nm, representative of accumulation mode, also to facilitate comparisons with the results reported by Reddington et al. (2011). We also used measurements by a TSI 3786 Condensational Particle Counter (CPC) aboard the FAAM BAe-146 aircraft measuring the number concentrations of particles larger than 4 nm.

A map of flight tracks by the Falcon 20 and Bae-146 and more details about EUCAARI-LONGREX dataset is available elsewhere (Reddington et al., 2011; Hamburger et al., 2012). Measurements from the LONGREX campaign span altitudes corresponding to 13 of the 14 vertical layers of PMCAMx-UF (Fig. S1 in the supplement). The model data were paired with the aircraft data by converting the time-dependent latitude, longitude, and altitude of the plane to a model grid-cell index.

3 Results

3.1 Surface-level particle number concentrations

In this study we explore the sensitivity of PMCAMx-UF to (1) updated NPF scheme with ACDC-based formation rates, (2) updated cloud adjustment scheme with TUV implementation, and (3) including natural particle number emissions. The baseline simulation (hereafter ACDC-TUV-DE; see Table 1) represents a prediction of the particle number concentrations with implementation of ACDC-based NPF scheme and TUV cloud adjustment scheme while using the default (i.e. only anthropogenic) particle emissions similarly to Fountoukis et al. (2012). Table 1 summarizes the simulations reported in this study. Figure 1 shows the arithmetic mean number concentration over May 2008 at ground-level for each PMCAMx-UF grid cell for particles larger than 10 (N_{10}), 50 (N_{50}) and 100 (N_{100}) nm and all particles (N_{tot}) as predicted using the baseline simulation ACDC-TUV-DE. The first two days of the simulation were excluded from the analysis to minimize the impact of the initial conditions on the results. The domain mean during May 2008 for N_{tot} is 59200 cm^{-3}, for N_{10} the corresponding number is 7100 cm^{-3}, for N_{50} 1300 cm^{-3}, and for N_{100} 360 cm^{-3}. The spatial pattern of the predicted number concentrations is similar to the results reported by Fountoukis et al. (2012), which were obtained using the simulation Napari-RADM-DE. The highest number concentrations are predicted over Eastern Europe during this photochemically active period while the lowest particle number concentrations are predicted over Nordic countries. The simulation Napari-TUV-DE predicts the domain mean of N_{tot}, N_{10}, N_{50} and N_{100} of 8100, 4000, 1500 and 410, respectively. Although updating the NPF scheme of PMCAMx-UF with ACDC-based formation rates significantly affects the number of small particles with diameter below 10 nm, the spatial concentration remains unchanged. Updating the model cloudiness scheme by

Geosci. Model Dev. Discuss., doi:10.5194/gmd-2016-21, 2016
Manuscript under review for journal Geosci. Model Dev.
Published: 11 February 2016
© Author(s) 2016. CC-BY 3.0 License.

Geoscientific Model Development Discussions

implementing the TUV radiative transfer module did not greatly affect the spatial distribution of number concentrations but caused a minor change in the number concentration values. This is confirmed by the arithmetic domain mean values during May 2008 of N_{tot}, N_{10}, N_{50} and N_{100} predicted by the ACDC-RADM-DE simulation, which are 62000, 6800, 1200 and 340 cm^{-3}, respectively, and thus very similar to the baseline simulation. Including the natural particle emissions (in simulation ACDC-TUV-NE) resulted in 48300, 6200, 1300 and 380 cm^{-3} for N_{tot}, N_{10}, N_{50} and N_{100}, respectively, therefore predicting lower number concentrations of small particles (i.e. diameter < 10 nm) compared to that predicted by the baseline simulation. This is probably due to the higher sink of newly formed particles caused by the added natural particle emissions.

Figure 2 shows scatter plots of the predicted (ACDC-RADM-DE) versus measured hourly-averaged N_{10}, N_{50} and N_{100} at the seven EUSAAR measurement sites during May 2008. More than 70 % of the data points for N_{50} and N_{100} predictions fall generally within a factor of two of the measurements, with slight underpredictions for N_{100} (38% below the 2:1 line) at some sites, similar to the results predicted by Napari-RADM-DE simulation reported by Fountoukis et al. (2012). However, the model using the ACDC-based formation rates is overpredicting $N_{10,}$ in particular over clean locations including Aspvreten, Hyytiälä, Vavihill and Mace Head. The reason for this overprediction is most likely linked to the missing condensable vapors and particle growth mechanisms in the simulations reported here (see Fountoukis et al., 2012; Ahlm et al., 2013; Patoulias et al., 2015). When implemented, the additional growth would likely increase the condensation sink by shifting the size distribution towards larger sizes. However, given the fact that no empirical fitting parameters have been applied to the ACDC-based NPF description, we deem the agreement encouraging. The biases presented here and in the following figures can thus be considered conservative estimates. Furthermore, in this study we have only considered the ternary sulfuric acid - water - ammonia particle formation scheme. There may be other significant mechanisms present, e.g. sulfuric acid - amine particle formation (Bergman et al., 2015), with a geographical pattern resembling that of our results. Both mechanisms depend on sulfuric acid concentration, the model prediction of which can naturally be inaccurate as well. We compared the modeled and measured acid concentrations at one of the measurement sites (Melpitz), and found that the modeled concentrations were slightly overpredicted (Fig. S2 in the supplement). This may also contribute to the overprediction of the small particle sizes.

3.2 Vertical profiles of particle number concentrations

In this section we investigate the vertical distribution of the means of N_{tot}, N_{10}, N_{50} and N_{100} along with parameters relevant for predicting NPF for the base case simulations (Fig. 3). These parameters include gas-phase concentrations of H_2SO_4 and NH_3, RH and T. In the results shown in Fig 3 the TUV radiation scheme has been used, thus representing the baseline simulation ACDC-TUV-DE. As can be seen from

Geosci. Model Dev. Discuss., doi:10.5194/gmd-2016-21, 2016
Manuscript under review for journal Geosci. Model Dev.
Published: 11 February 2016
© Author(s) 2016. CC-BY 3.0 License.

Fig. 3, particles smaller than 10 nm contribute significantly to the total number concentration throughout the tropospheric column, N_{tot} is about one order of magnitude greater than N_{10} and two and three orders of magnitudes greater than N_{50} and N_{100}, respectively. Values of N_{10}, N_{50} and N_{100} decrease monotonically with altitude, dropping significantly at approximately 1 km (layers 6-8 of the model). The vertical distribution of N_{tot} shows a different trend at higher altitudes where a bump in N_{tot} occurs at around 6-11 km, although no significant increase in the gas phase concentration of H_2SO_4 and NH_3 are predicted at these altitudes (Fig. 3). The increase in N_{tot} is mostly due to significantly decreased coagulation sink for the newly-formed particles, as the number of larger particles dramatically decreases with altitude, and partly due to the rapidly decreasing temperature. PMCAMx-UF predicts the particle formation rates to decrease rapidly from around 2 km upward. The temperature, RH and sulfuric acid profile have similar relative trends as the N_{10}, N_{50} and N_{100} profiles. There is a plateau in temperature and RH (at temperature range 285-288 K and RH range 80-83 %) profile up to altitude 1.2 km. Above this altitude, however, the RH and temperature values decrease rapidly. The sharp decreases in the relative humidity, temperature and particle number concentrations are consistent with the location of the boundary layer height. This is in agreement with Ferrero et al., (2010) who showed that mixing height estimations (over the city of Milan) derived from particle number concentration, temperature and relative humidity are correlated with one another.

Figure 4 shows the comparison of the two simulations ACDC-TUV-DE and Napari-TUV-DE (see Table 1) with the observational data collected during the EUCAARI-LONGREX campaign measured by German DLR Falcon 20 and the British FAAM BAe-146 aircraft. The model using the ACDC-based formation rates predicts the number concentration profile of particles larger than 4 nm (N_4) within about one order of magnitude of the observed N_4 profile throughout the atmospheric column. The scaled Napari NPF scheme leads to N_4 concentrations somewhat closer to the observations than those using the ACDC scheme. As mentioned above, the vertical profiles presented in Figure 4 are produced by the model using the TUV radiation scheme. A similar analysis of the vertical profiles using the RADM radiation scheme (simulation ACDC-RADM-DE), which is not shown here, results in exactly the same shape of the number concentration profiles. The vertical profiles using the RADM radiation scheme show negligible difference in the absolute number concentrations with slightly worse agreement with the observations compared to the TUV radiation scheme. The number concentrations of particles larger than 10 nm (N_{10}) predicted by the model using the scaled Napari NPF scheme agrees reasonably well with the observations throughout the atmospheric column. The model using the ACDC formation rates tends to slightly overpredict the N_{10} profile. The shape of the observed N_{10} vertical profile is captured reasonably well throughout the atmospheric column regardless of the NPF scheme used. Both model versions have almost the same performance for the $N_{160\text{-}1040}$ profile within the boundary layer; both simulations (i.e. ACDC-TUV-DE and Napari-TUV-DE) underpredicting the $N_{160\text{-}1040}$ profile by about half an order of magnitude. This behavior is seen in the $N_{160\text{-}1040}$ profile corresponding to both

Geosci. Model Dev. Discuss., doi:10.5194/gmd-2016-21, 2016
Manuscript under review for journal Geosci. Model Dev.
Published: 11 February 2016
© Author(s) 2016. CC-BY 3.0 License.

observational data sets (i.e. Falcon 20 (Fig. 4-d) and BAe 146 (Fig 4-e) aircraft data). This is at least partly due to the lack of sources of organic condensable vapors to grow the particles to larger sizes in the model (Patoulias et al., 2015), which will be investigated in a future study. The underprediction decreases for all model versions at altitudes above the boundary layer improving the agreement with observational data.

The results for the model using the ACDC-based formation rates are comparable to previous studies. For example, Reddington et al. (2011) tested different NPF parameterizations in BL including activation, kinetic and combined organic-H_2SO_4 parameterizations, which are implemented in the Global Model of Aerosol Processes (GLOMAP). The evaluation of the modeled vertical profiles of particle number concentrations against the aircraft measurements similar to this study showed that all of the mentioned NPF schemes dramatically under-predicted particles in nucleation (normalized mean bias (NMB) varies from -33 to -96) and Aitken mode sizes (-44 < NMB < -59). The larger particles (N_{100}) however were generally well-captured by the model. Furthermore, Lupascu et al. (2015) compared simulated number concentrations with aircraft measurements collected during the Carbonaceous Aerosol and Radiative Effects Study (CARES) campaign. They also tested different NPF parameterizations including activation, kinetic and combined organic-H_2SO_4 parameterizations, which are implemented in the regional scale model WRF-Chem one-at-a-time using a sectional framework to simulate the NPF. They found that their simulations overpredicted the particle number concentrations, especially in the smallest sizes (normalized mean bias of 126-608 % for N_3 and N_{10}). The nucleation scheme had very little impact on the magnitude of the CCN-sized particle number concentrations.

3.3 Effect of the radiative transfer scheme on predictions of particle number concentrations

Updating the radiative transfer scheme to the TUV scheme has a small effect on the predicted number concentrations; the vertical profile of the relative difference (N_{TUV} - N_{RADM}) × 100 / N_{RADM} in the May-2008 domain mean particle number concentrations shows a maximum reduction of about -5.5 % in N_{tot} (at altitude 2.2 km) and a maximum increase of about 9 % in N_{100} (at altitude range 0.7-2.2 km). Figure 5 shows the spatial distribution of the absolute difference of the H_2SO_4 gas phase concentration and total particle number concentrations between the simulations ACDC-TUV-DE and ACDC-RADM-DE (see Table 1) at 12:00 UTC on May 5, 2008. Figure 5 also presents the cloud optical depth fields to illustrate the link between the cloud fields and changes in the particle number concentrations due to the new cloud adjustment scheme. The TUV scheme results in higher particle formation rates above and in the vicinity of the cloudy regions due to enhanced radiation and sulfuric acid production. This is in agreement with observations reported by Wehner et al. (2015). They concluded that the cloudy regions provide a favorable environment for NPF above and at the edges of clouds due to enhanced upward spectral irradiance and cloud-reflected spectral radiance around them. Sulfuric acid concentration is reduced

Geosci. Model Dev. Discuss., doi:10.5194/gmd-2016-21, 2016
Manuscript under review for journal Geosci. Model Dev.
Published: 11 February 2016
© Author(s) 2016. CC-BY 3.0 License.

below cloud in the TUV scheme, due to the enhanced UV attenuation scaling down the photolysis rates. However, as pointed out above, the effect on the total particle number concentrations is generally small.

4 Conclusions

We have updated the new particle formation (NPF) scheme within PMCAMx-UF with particle formation rates for the ternary H_2SO_4-NH_3-H_2O pathway simulated by the Atmospheric Cluster Dynamics Code using quantum chemical input data. The ACDC results were implemented in PMCAMx-UF as a lookup table from which the formation rates were interpolated. We believe this is the first time that reasonable particle concentrations have been produced in a large-scale atmospheric model with a NPF scheme without any scaling factors or location/condition dependent semi-empiricism. In addition to the updated NPF description, we have also updated PMCAMx-UF treatment of the cloudiness effect on the photolysis rates (i.e. cloud adjustment scheme) profile by implementing a streamlined version of the Tropospheric Ultraviolet and Visible radiative transfer model (Madronich, 2002).

We used the updated PMCAMx-UF to simulate particle number concentration during May 2008 over Europe. During this period, the EUCAARI campaign was performed to measure the particle number size distributions within the atmospheric boundary layer at various European Supersites for Atmospheric Aerosol Research (EUSAAR) in addition to higher altitude data collected by two research aircraft during the LONGREX campaign. Comparing the measured particle number concentrations at the EUSAAR sites to the predictions of the updated PMCAMx-UF shows that the model slightly overpredicts concentrations for particles with diameters between 10-100 nm. Particles larger than 100 nm are slightly underpredicted. In general, the model predictions of number concentrations of aerosols, in particular particles within Aitken and accumulation mode sizes agree reasonably well with the measurements.

Vertical profiles of particle number concentrations show that predicted concentrations of small particles are within one order of magnitude of the aircraft measurements. The predicted Aitken- and accumulation mode number concentrations are in quite good agreement with the observational data throughout the atmospheric column, while the concentrations of smaller particles are somewhat overpredicted by the ACDC-based NPF scheme. Including organic condensation onto the ultrafine particles could improve these predictions.

Overall, we consider our results very promising: a NPF scheme based on first-principles theory and no artificial scaling is shown to be a promising alternative to semi-empirical approaches in the description of particle formation in large scale atmospheric models.

Geosci. Model Dev. Discuss., doi:10.5194/gmd-2016-21, 2016
Manuscript under review for journal Geosci. Model Dev.
Published: 11 February 2016
© Author(s) 2016. CC-BY 3.0 License.

Geoscientific Model Development Discussions
Open Access
EGU

Code availability

The look-up table used for the representation of particle formation rates is openly available for download at http://www.aces.su.se/research/research-facilities/models. The updated NPF and TUV modules are available from I. Riipinen (ilona.riipinen@aces.su.se).

Acknowledgements

We gratefully acknowledge Oona Kupiainen-Määttä for providing the ACDC-simulation data and generating the look-up table. Tinja Olenius is acknowledged for discussions and technical support related to ACDC, and Radovan Krejci for providing the EUCAARI-LONGREX data. Falcon measurements and data analysis were funded by EUCAARI (European Integrated project on Aerosol Cloud Climate and Air Quality interactions) project No. 036833-2 and by DLR. The UK aircraft experiment was supported through EUCAARI and the UK Natural Environment Research Council through the APPRAISE programme, grant NE/E01108X/1. The authors also thank the Academy of Finland Center of Excellence program (project number 272041), the Nordic Centre of Excellence CRAICC , Academy of Finland, ERC-StG-ATMOGAIN (278277) and ERC-StG_MOCAPAF (257360).

References

Ahlm, L., Julin, J., Fountoukis, C., Pandis, S. N., and Riipinen, I.: Particle number concentrations over Europe in 2030: the role of emissions and new particle formation, Atmos. Chem. Phys., 13, 10271-10283, doi:10.5194/acp-13-10271-2013, 2013.

Adams, P. J., and J. H. Seinfeld, Predicting global aerosol size distributions in general circulation models, J. Geophys. Res., 107, 4370, doi:10.1029/2001JD001010, 2002.

Almeida, J., Schobesberger, S., Kürten, A., Ortega, I. K., Kupiainen-Määttä, O., Praplan, A. P., Adamov, A., Amorim, A., Bianchi, F., Breitenlechner, M., David, A., Dommen, J., Donahue, N. M., Downard, A., Dunne, E., Duplissy, J., Ehrhart, S., Flagan, R. C., Franchin, A., Guida, R., Hakala, J., Hansel, A., Heinritzi, M., Henschel, H., Jokinen, T., Junninen, H., Kajos, M., Kangasluoma, J., Keskinen, H., Kupc, A., Kurtén, T., Kvashin, A. N., Laaksonen, A., Lehtipalo, K., Leiminger, M., Leppä, J., Loukonen, V., Makhmutov, V., Mathot, S., McGrath, M. J., Nieminen, T., Olenius, T., Onnela, A., Petäjä, T., Riccobono, F., Riipinen, I., Rissanen, M., Rondo, L., Ruuskanen, T., Santos, F. D., Sarnela, N., Schallhart, S., Schnitzhofer, R., Seinfeld, J. H., Simon, M., Sipilä, M., Stozhkov, Y., Stratmann, F., Tomé, A., Tröstl, J., Tsagkogeorgas, G., Vaattovaara, P., Viisanen, Y., Virtanen, A., Vrtala, A., Wagner, P. E., Weingartner, E., Wex, H., Williamson, C., Wimmer, D., Ye, P., Yli-Juuti, T., Carslaw, K. S., Kulmala, M., Curtius, J., Baltensperger, U., Worsnop, D. R., Vehkamäki, H., and Kirkby, J: Molecular understanding of sulphuric acid-amine particle nucleation in the atmosphere. Nature, 502: 359-363, doi:10.1038/nature12663, 2013.

Asmi, A., Wiedensohler, A., Laj, P., Fjaeraa, A.-M., Sellegri, K., Birmili, W., Weingartner, E., Baltensperger, U., Zdimal, V., Zikova, N., Putaud, J.-P., Marinoni, A., Tunved, P., Hansson, H.-C., Fiebig, M., Kivekäs, N.,

© Author(s) 2016. CC-BY 3.0 License.

496 Lihavainen, H., Asmi, E., Ulevicius, V., Aalto, P. P., Swietlicki, E., Kristensson, A., Mihalopoulos, N., Kalivitis,
497 N., Kalapov, I., Kiss, G., de Leeuw, G., Henzing, B., Harrison, R. M., Beddows, D., O'Dowd, C., Jennings, S. G.,
498 Flentje, H., Weinhold, K., Meinhardt, F., Ries, L., and Kulmala, M.: Number size distributions and seasonality of
499 submicron particles in Europe 2008–2009, Atmos. Chem. Phys., 11, 5505-5538, doi:10.5194/acp-11-5505-2011,
500 2011.
501
502 Bergman, T., A. Laaksonen, H. Korhonen, J. Malila, E. M. Dunne, T. Mielonen, K. E. J. Lehtinen, T. Kühn, A.
503 Arola, and H. Kokkola (2015) Geographical and Diurnal Features of Amine-Enhanced Boundary Layer Nucleation
504 J. Geophys. Res. Atmos., 120, 9606–9624.
505
506 Chang, J. S., Brost, R. A., Isaksen, I. S. A., Madronich, S., Middleton, P., Stockwell, W. R., and Walcek, C. J.: A
507 three-dimensional Eulerian acid deposition model: Physical concepts and formulation, J. Geophys. Res., 92(D12),
508 14681–14700, doi:10.1029/JD092iD12p14681, 1987.
509
510 Cui, Z., Gadian, A., Blyth, A., Crosier, J., and Crawford, I.: Observations of the Variation in Aerosol and Cloud
511 Microphysics along the 20°S Transect on 13 November 2008 during VOCALS-Rex, J. Atmos. Sci., 71, 2927–
512 2943, doi: http://dx.doi.org/10.1175/JAS-D-13-0245.1, 2014.
513
514 Dal Maso, M., Kulmala, M., Lehtinen, K. E. J., Mäkelä, J. M., Aalto, P., and O'Dowd, C. D.: Condensation and
515 coagulation sinks and formation of nucleation mode particles in coastal and boreal forest boundary layers, J.
516 Geophys. Res., 107(D19), doi:10.1029/2001JD001053, 2002.
517
518 Denier van der Gon, H. A. C., Visschedijk, A. J. H., Johansson, C., Hedberg Larsson, E., Harrison, R., and
519 Beddows, D.: Size resolved pan European anthropogenic particle number inventory, EUCAARI Deliverable report
520 D141 (available on request from EUCAARI project office), 2009.
521
522 Emery, C., J. Jung, J. Johnson, G. Yarwood, and D. Boyer: Improving cloud impacts on photolysis using an on-
523 line radiation model in CAMx, presented at the 9th Annual CMAS Conference, pp. 9–14, 2010.
524
525 Ferrero, L., Perrone, M. G., Petraccone, S., Sangiorgi, G., Ferrini, B. S., Lo Porto, C., Lazzati, Z., Cocchi, D.,
526 Bruno, F., Greco, F., Riccio, A., and Bolzacchini, E.: Vertically-resolved particle size distribution within and above
527 the mixing layer over the Milan metropolitan area, Atmos. Chem. Phys., 10, 3915-3932, doi:10.5194/acp-10-3915-
528 2010, 2010.
529
530 Fahey K. M., and Pandis, S. N.: Optimizing model performance: Variable size resolution in cloud chemistry
531 modeling, Atmos. Environ., 35, 4471-4478, doi:10.1016/S1352-2310(01)00224-2, 2001.
532
533 Feldpausch, P., Fiebig, M., Fritzsche, L., and Petzold, A.: Measurement of ultrafine aerosol size distributions by a
534 combination of diffusion screen separators and condensation particle counters, J.Aerosol Sci., 37, 577–597,
535 doi:10.1016/j.jaerosci.2005.04.009, 2006.
536
537 Fiebig, M., Stein, C., Schroder, F., Feldpausch, P., and Petzold, A.: Inversion of data containing information on the
538 aerosol particle size distribution using multiple instruments, J. Aerosol Sci., 36, 1353–1372,
539 doi:10.1016/j.jaerosci.2005.01.004, 2005.
540
541 Fountoukis, C., Racherla, P. N., Denier van der Gon, H. A. C., Polymeneas, P., Charalampidis, P. E., Pilinis, C.,
542 Wiedensohler, A., Dall'Osto, M., O'Dowd, C., and Pandis, S. N.: Evaluation of a three-dimensional chemical
543 transport model (PMCAMx) in the European domain during the EUCAARI May 2008 campaign, Atmos. Chem.
544 Phys., 11, 10331-10347, doi:10.5194/acp-11-10331-2011, 2011.
545
546 Fountoukis, C., Riipinen, I., Denier van der Gon, H. A. C., Charalampidis, P. E., Pilinis, C., Wiedensohler, A.,
547 O'Dowd, C., Putaud, J. P., Moerman, M., and Pandis, S. N.: Simulating ultrafine particle formation in Europe

© Author(s) 2016. CC-BY 3.0 License.

548 using a regional CTM: contribution of primary emissions versus secondary formation to aerosol number
549 concentrations, Atmos. Chem. Phys., 12, 8663-8677, doi:10.5194/acp-12-8663-2012, 2012.
550
551 Fuzzi, S., Baltensperger, U., Carslaw, K., Decesari, S., Denier van der Gon, H., Facchini, M. C., Fowler, D.,
552 Koren, I., Langford, B., Lohmann, U., Nemitz, E., Pandis, S., Riipinen, I., Rudich, Y., Schaap, M., Slowik, J. G.,
553 Spracklen, D. V., Vignati, E., Wild, M., Williams, M., and Gilardoni, S.: Particulate matter, air quality and climate:
554 lessons learned and future needs, Atmos. Chem. Phys., 15, 8217-8299, doi:10.5194/acp-15-8217-2015, 2015.
555
556 Gaydos, T. M., Stanier, C. O., and Pandis, S. N.: Modelling of in situ ultrafine atmospheric particle formation in
557 the eastern United States, J. Geophys. Res., 110, D07S12, doi:10.1029/2004JD004683, 2005.
558
559 Gaydos, T., Pinder, R., Koo, B., Fahey, K., Yarwood, G., and Pandis, S. N.: Development and application of a
560 three-dimensional aerosol chemical transport model, PMCAMx, Atmos. Environ., 41, 2594–2611,
561 doi:10.1016/j.atmosenv.2006.11.034, 2007.

562 Guenther, A., Karl, T., Harley, P., Wiedinmyer, C., Palmer, P. I., and Geron, C.: Estimates of global terrestrial
563 isoprene emissions using MEGAN (Model of Emissions of Gases and Aerosols from Nature), Atmos. Chem.
564 Phys., 6, 3181-3210, doi:10.5194/acp-6-3181-2006, 2006.

565 Hamburger, T., McMeeking, G., Minikin, A., Birmili, W., Dall'Osto, M., O'Dowd, C., Flentje, H., Henzing, B.,
566 Junninen, H., Kristensson, A., de Leeuw, G., Stohl, A., Burkhart, J. F., Coe, H., Krejci, R., and Petzold, A.:
567 Overview of the synoptic and pollution situation over Europe during the EUCAARI-LONGREX field campaign,
568 Atmos. Chem. Phys., 11, 1065-1082, doi:10.5194/acp-11-1065-2011, 2011.
569
570 Hamburger, T., McMeeking, G., Minikin, A., Petzold, A., Coe, H., and Krejci, R.: Airborne observations of aerosol
571 microphysical properties and particle ageing processes in the troposphere above Europe, Atmos. Chem. Phys., 12,
572 11533-11554, doi:10.5194/acp-12-11533-2012, 2012.
573
574 Henschel, H., Navarro, J. C. A., Yli-Juuti, T., Kupiainen-Määttä, O., Olenius, T., Ortega, I. K., Clegg, S. L.,
575 Kurtén, T., Riipinen, I., and Vehkamäki, H.: Hydration of atmospherically relevant molecular clusters:
576 Computational chemistry and classical thermodynamics. J. Phys. Chem. A., 118: 2599-2611,
577 doi:10.1021/jp500712y, 2014.
578
579 Henschel, H., Kurtén, T., and Vehkamäki, H.: A computational study on the effect of hydration on new particle
580 formation in the sulfuric acid/ammonia and sulfuric acid/dimethylamine systems, submitted to Journal of Physical
581 Chemistry, 2015
582
583 Jen, C. N., P. H. McMurry, and D. R. Hanson: Stabilization of sulfuric acid dimers by ammonia, methylamine,
584 dimethylamine, and trimethylamine, J. Geophys. Res., 119, 7502–7514, doi:10.1002/2014JD021592, 2014.
585
586 Jung, J., Adams, P. J., and Pandis, S. N.: Simulating the size distribution and chemical composition of ultrafine
587 particles during nucleation events.Atmospheric Environment, 40(13), 2248-2259,
588 doi:10.1016/j.atmosenv.2005.09.082, 2006.
589
590 Jung, J. G., Pandis, S. N., and Adams, P. J.: Evaluation of nucleation theories in a sulfur-rich environment. Aerosol
591 Sci. Technol., 42(7), 495-504, doi:10.1080/02786820802187085, 2008.
592
593 Jung, J., Fountoukis, C., Adams, P. J., and Pandis, S. N.: Simulation of in situ ultrafine particle formation in the
594 eastern United States using PMCAMx-UF, J. Geophys. Res., 115, D03203, doi:10.1029/2009JD012313, 2010.
595
596 Karydis, V. A., Tsimpidi, A. P., and Pandis, S. N.: Evaluation of a three-dimensional chemical transport model
597 (PMCAMx) in the eastern United States for all four seasons, J. Geophys. Res., 112, D14211,
598 doi:10.1029/2006JD007890, 2007.

© Author(s) 2016. CC-BY 3.0 License.

599
600 Kerminen, V.-M., Paramonov, M., Anttila, T., Riipinen, I., Fountoukis, C., Korhonen, H., Asmi, E., Laakso, L.,
601 Lihavainen, H., Swietlicki, E., Svenningsson, B., Asmi, A., Pandis, S. N., Kulmala, M., and Petäjä, T.: Cloud
602 condensation nuclei production associated with atmospheric nucleation: a synthesis based on existing literature
603 and new results, Atmos. Chem. Phys., 12, 12037-12059, doi:10.5194/acp-12-12037-2012, 2012.
604
605 Kirkby, J., Curtius, J., Almeida, J., Dunne, E., Duplissy, J., Ehrhart, S., Franchin, A., Gagné, S., Ickes, L., Kürten,
606 A., Kupc, A., Metzger, A., Riccobono, F., Rondo, L., Schobesberger, S., Tsagkogeorgas, G., Wimmer, D.,
607 Amorim, A., Bianchi, F., and Breitenlechner, M.: Role of sulphuric acid, ammonia and galactic cosmic rays in
608 atmospheric aerosol nucleation, Nature 476, 429-433, doi:10.1038/nature10343, 2011.

609 Korhonen, P., Kulmala, M., Laaksonen, A., Viisanen, Y., McGraw, R. and Seinfeld, J. H.: Ternary nucleation of
610 H_2SO_4, NH_3, and H_2O in the atmosphere, J. Geophys. Res., 104, 26349–26353, doi:10.1029/1999JD900784, 1999.
611
612 Kulmala, M., Liisa, P, and Mäkelä, J. M.: Stable sulphate clusters as a source of new atmospheric
613 particles, *Nature* 404, no. 6773, 66-69, doi: 10.1038/35003550, 2000.
614
615 Kulmala, M., Vehkamäki, H., Petäjä, T., Dal Maso, M., Lauri, A., Kerminen, V.-M., Birmili, and W., McMurry,
616 P.H.: Formation and growth rates of ultrafine atmospheric particles: a review of observations, J Aerosol Sci.,
617 35:143-76, doi:10.1016/j.jaerosci.2003.10.003, 2004.
618
619 Kulmala, M., Lehtinen, K. E. J., and Laaksonen, A.: Cluster activation theory as an explanation of the linear
620 dependence between formation rate of 3 nm particles and sulphuric acid concentration, Atmos. Chem. Phys., 6,
621 787–793, doi:10.5194/acp-6-787-2006, 2006.
622
623 Kulmala, M., Asmi, A., Lappalainen, H. K., Carslaw, K. S., Pöschl, U., Baltensperger, U., Hov, Ø., Brenquier, J.-
624 L., Pandis, S. N., Facchini, M. C., Hansson, H.-C., Wiedensohler, A., and O'Dowd, C. D.: Introduction: European
625 Integrated Project on Aerosol Cloud Climate and Air Quality interactions (EUCAARI) – integrating aerosol
626 research from nano to global scales, Atmos. Chem. Phys., 9, 2825-2841, doi:10.5194/acp-9-2825-2009, 2009.
627
628 Kulmala, M., Asmi, A., Lappalainen, H. K., Baltensperger, U., Brenguier, J.-L., Facchini, M. C., Hansson, H.-C.,
629 Hov, Ø., O'Dowd, C. D., Pöschl, U., Wiedensohler, A., Boers, R., Boucher, O., de Leeuw, G.,
630 Denier van der Gon, H. A. C., Feichter, J., Krejci, R., Laj, P., Lihavainen, H., Lohmann, U., McFiggans, G.,
631 Mentel, T., Pilinis, C., Riipinen, I., Schulz, M., Stohl, A., Swietlicki, E., Vignati, E., Alves, C., Amann, M.,
632 Ammann, M., Arabas, S., Artaxo, P., Baars, H., Beddows, D. C. S., Bergström, R., Beukes, J. P., Bilde, M.,
633 Burkhart, J. F., Canonaco, F., Clegg, S. L., Coe, H., Crumeyrolle, S., D'Anna, B., Decesari, S., Gilardoni, S.,
634 Fischer, M., Fjaeraa, A. M., Fountoukis, C., George, C., Gomes, L., Halloran, P., Hamburger, T., Harrison, R. M.,
635 Herrmann, H., Hoffmann, T., Hoose, C., Hu, M., Hyvärinen, A., Hõrrak, U., Iinuma, Y., Iversen, T., Josipovic, M.,
636 Kanakidou, M., Kiendler-Scharr, A., Kirkevåg, A., Kiss, G., Klimont, Z., Kolmonen, P., Komppula, M.,
637 Kristjánsson, J.-E., Laakso, L., Laaksonen, A., Labonnote, L., Lanz, V. A., Lehtinen, K. E. J., Rizzo, L. V.,
638 Makkonen, R., Manninen, H. E., McMeeking, G., Merikanto, J., Minikin, A., Mirme, S., Morgan, W. T.,
639 Nemitz, E., O'Donnell, D., Panwar, T. S., Pawlowska, H., Petzold, A., Pienaar, J. J., Pio, C., Plass-Duelmer, C.,
640 Prévôt, A. S. H., Pryor, S., Reddington, C. L., Roberts, G., Rosenfeld, D., Schwarz, J., Seland, Ø., Sellegri, K.,
641 Shen, X. J., Shiraiwa, M., Siebert, H., Sierau, B., Simpson, D., Sun, J. Y., Topping, D., Tunved, P., Vaattovaara, P.,
642 Vakkari, V., Veefkind, J. P., Visschedijk, A., Vuollekoski, H., Vuolo, R., Wehner, B., Wildt, J., Woodward, S.,
643 Worsnop, D. R., van Zadelhoff, G.-J., Zardini, A. A., Zhang, K., van Zyl, P. G., Kerminen, V.-M., S Carslaw, K.,
644 and Pandis, S. N.: General overview: European Integrated project on Aerosol Cloud Climate and Air Quality
645 interactions (EUCAARI) – integrating aerosol research from nano to global scales, Atmos. Chem. Phys., 11,
646 13061-13143, doi:10.5194/acp-11-13061-2011, 2011.
647
648 Laaksonen, A., Kulmala, M., Berndt, T., Stratmann, F., Mikkonen, S., Ruuskanen, A., Lehtinen, K. E. J.,
649 Dal Maso, M., Aalto, P., Petäjä, T., Riipinen, I., Sihto, S.-L., Janson, R., Arnold, F., Hanke, M., Ücker, J.,
650 Umann, B., Sellegri, K., O'Dowd, C. D., and Viisanen, Y.: SO_2oxidation products other than H_2SO_4 as a trigger of

© Author(s) 2016. CC-BY 3.0 License.

651 new particle formation. Part 2: Comparison of ambient and laboratory measurements, and atmospheric
652 implications, Atmos. Chem. Phys., 8, 7255-7264, doi:10.5194/acp-8-7255-2008, 2008.
653
654 Liu , P. S. K., Leaitch , W. R. , Strapp, J. W., and Wasey, M. A.: Response of Particle Measuring Systems Airborne
655 ASASP and PCASP to NaCl and Latex Particles, Aerosol Sci. Technol., 16, 83-95,
656 doi:0.1080/02786829208959539, 1992.
657
658 Lupascu, A., Easter, R., Zaveri, R., Shrivastava, M., Pekour, M., Tomlinson, J., Yang, Q., Matsui, H., Hodzic, A.,
659 Zhang, Q., and Fast, J. D.: Modeling particle nucleation and growth over northern California during the 2010
660 CARES campaign, Atmos. Chem. Phys. Discuss., 15, 19729-19801, doi:10.5194/acpd-15-19729-2015, 2015.
661
662 Madronich, S., National Center for Atmospheric Research, Boulder, Colorado, (2002). Tropospheric ultraviolet
663 and visible radiation model. [Available online at http://acd.ucar.edu/models/UV/TUV/index.html.]
664
665 Makkonen, R., Asmi, A., Korhonen, H., Kokkola, H., Järvenoja, S., Räisänen, P., Lehtinen, K. E. J., Laaksonen, A.,
666 Kerminen, V.-M., Järvinen, H., Lohmann, U., Bennartz, R., Feichter, J., and Kulmala, M.: Sensitivity of aerosol
667 concentrations and cloud properties to nucleation and secondary organic distribution in ECHAM5-HAM global
668 circulation model, Atmos. Chem. Phys., 9, 1747-1766, doi:10.5194/acp-9-1747-2009, 2009.
669
670 Matsui, H., M. Koike, Y. Kondo, N. Takegawa, A. Wiedensohler, J. D. Fast, and R. A. Zaveri: Impact of new
671 particle formation on the concentrations of aerosols and cloud condensation nuclei around Beijing, J. Geophys.
672 Res., 116, D19208, doi:10.1029/2011JD016025, 2011a.
673
674 Matsui, H., M. Koike, N. Takegawa, Y. Kondo, A. Takami, T. Takamura, S. Yoon, S.-W. Kim, H.-C. Lim, and J.
675 D. Fast: Spatial and temporal variations of new particle formation in East Asia using an NPF-explicit WRF-chem
676 model: North-south contrast in new particle formation frequency, J. Geophys. Res. Atmos., 118, 11,647–11,663,
677 doi:10.1002/jgrd.50821, 2013c.
678
679 McMurry, P.: Photochemical aerosol formation from SO_2: A theoretical analysis of smog chamber data, J. Colloid
680 Interface Sci., 78(2), 513–527, doi:10.1016/0021-9797(80)90589-5, 1980.
681
682 Merikanto, J., Spracklen, D. V., Mann, G. W., Pickering, S. J., and Carslaw, K. S.: Impact of nucleation on global
683 CCN, Atmos. Chem. Phys., 9, 8601-8616, doi:10.5194/acp-9-8601-2009, 2009.
684
685 Merikanto J., Zapadinsky E., Lauri A., Vehkamäki H.: Origin of the Failure of Classical Nucleation Theory:
686 Incorrect Description of the Smallest Clusters, Phys. Rev. Lett., 98, 145702, doi:10.1103/PhysRevLett.98.145702,
687 2007a.
688
689 Merikanto, J., I. Napari, H. Vehkamäki, T. Anttila, and M. Kulmala: New parameterization of sulfuric acid-
690 ammonia-water ternary nucleation rates at tropospheric conditions, J. Geophys. Res., 112, D15207,
691 doi:10.1029/2006JD007977, 2007b.
692
693 Napari, I., Kulmala, M., and Vehkamaki, H.: Ternary nucleation of inorganic acids, ammonia, and water, J. Chem.
694 Phys., 117, 8418– 8425, doi:10.1063/1.1511722, 2002.
695
696 O'Dowd, C. D., B. Langmann, S. Varghese, C. Scannell, D. Ceburnis, and M. C. Facchini: A combined organic-
697 inorganic sea-spray source function, Geophys. Res. Lett., 35, L01801, doi:10.1029/2007GL030331, 2008.
698
699 Olenius, T., Kupiainen-Määttä, O., Ortega, I. K., Kurtén, T., and Vehkamäki, H.: Free energy barrier in the growth
700 of sulfuric acid–ammonia and sulfuric acid–dimethylamine clusters, J. Chem. Phys., 139: 084312,
701 doi:10.1063/1.4819024, 2013.
702

© Author(s) 2016. CC-BY 3.0 License.

703 Ortega, I. K., Kupiainen, O., Kurtén, T., Olenius, T., Wilkman, O., McGrath, M. J., Loukonen, V., and
704 Vehkamäki, H.: From quantum chemical formation free energies to evaporation rates, Atmos. Chem. Phys., 12,
705 225-235, doi:10.5194/acp-12-225-2012, 2012.
706
707 Paasonen, P., Nieminen, T., Asmi, E., Manninen, H. E., Petäjä, T., Plass-Dülmer, C., Flentje, H., Birmili, W.,
708 Wiedensohler, A., Hõrrak, U., Metzger, A., Hamed, A., Laaksonen, A., Facchini, M. C., Kerminen, V.-M., and
709 Kulmala, M.: On the roles of sulphuric acid and low-volatility organic vapours in the initial steps of atmospheric
710 new particle formation, Atmos. Chem. Phys., 10, 11223–11242, doi:10.5194/acp-10-11223-2010, 2010.
711
712 Patoulias, D., Fountoukis, C., Riipinen, I., and Pandis, S. N.: The role of organic condensation on ultrafine particle
713 growth during nucleation events, Atmos. Chem. Phys., 15, 6337-6350, doi:10.5194/acp-15-6337-2015, 2015.
714
715 Pierce, J. R. and Adams, P. J.: A computationally efficient aerosol nucleation/ condensation method:
716 pseudo-steady-state sulfuric acid, aerosol science and technology, 43:3, 216-226, doi:
717 10.1080/02786820802587896, 2009.
718
719 Reddington, C. L., Carslaw, K. S., Spracklen, D. V., Frontoso, M. G., Collins, L., Merikanto, J., Minikin, A.,
720 Hamburger, T., Coe, H., Kulmala, M., Aalto, P., Flentje, H., Plass-Dülmer, C., Birmili, W., Wiedensohler, A.,
721 Wehner, B., Tuch, T., Sonntag, A., O'Dowd, C. D., Jennings, S. G., Dupuy, R., Baltensperger, U., Weingartner, E.,
722 Hansson, H.-C., Tunved, P., Laj, P., Sellegri, K., Boulon, J., Putaud, J.-P., Gruening, C., Swietlicki, E., Roldin, P.,
723 Henzing, J. S., Moerman, M., Mihalopoulos, N., Kouvarakis, G., Ždímal, V., Zíková, N., Marinoni, A.,
724 Bonasoni, P., and Duchi, R.: Primary versus secondary contributions to particle number concentrations in the
725 European boundary layer, Atmos. Chem. Phys., 11, 12007-12036, doi:10.5194/acp-11-12007-2011, 2011.
726
727 Sihto, S.-L., Kulmala, M., Kerminen, V.-M., Dal Maso, M., Petäjä, T., Riipinen, I., Korhonen, H., Arnold, F.,
728 Janson, R., Boy, M., Laaksonen, A., and Lehtinen, K. E. J.: Atmospheric sulphuric acid and aerosol formation:
729 implications from atmospheric measurements for nucleation and early growth mechanisms, Atmos. Chem. Phys.,
730 6, 4079–4091, doi:10.5194/acp-6-4079-2006, 2006.
731
732 Skamarock, W. C., J. B. Klemp, J. Dudhia, D. O. Gill, D. M. Barker, and W. Wang: A Description of the Advanced
733 Research WRF Version 2, NCAR Technical Note
734 (http://opensky.ucar.edu/islandora/object/technotes%3A479/datastream/PDF/view), doi:10.5065/D6DZ069T,
735 2005.
736
737 Sofiev, M., Vankevich, R., Lanne, M., Koskinen, J., and Kukkonen, J.: On integration of a Fire Assimilation System
738 and a chemical transport model for near-real-time monitoring of the impact of wild-land fires on atmospheric
739 composition and air quality, Modelling, Monitoring and Management of Forest Fires, WIT Transactions on
740 Ecology and the Environment, 119, 343–351, 2008a.
741
742 Sofiev, M., Lanne, M., Vankevich, R., Prank, M., Karppinen, A., and Kukkonen, J.: Impact of wild-land fires on
743 European air quality in 2006–2008, Modelling, Monitoring and Management of Forest Fires, WIT Transactions
744 on Ecology and the Environment, 119, 353–361, 2008b.
745
746 Spracklen, D. V., Carslaw, K. S., Kulmala, M., Kerminen, V.-M., Mann, G. W., and Sihto, S.-L.: The contribution
747 of boundary layer nucleation events to total particle concentrations on regional and global scales, Atmos. Chem.
748 Phys., 6, 5631-5648, doi:10.5194/acp-6-5631-2006, 2006.
749
750 Takemura, T., T. Nakajima, O. Dubovik, B.N. Holben, S. Kinne: Single scattering albedo and radiative forcing of
751 various aerosol species with a global threedimensional model. J. Climate, 15, 333352, doi:10.1175/1520-
752 0442(2002)015<0333:SSAARF>2.0.CO;2, 2002.
753
754 Vehkamäki, H., Kulmala, M., Napari, I., Lehtinen, K. E. J., Timmreck, C., Noppel, M., and Laaksonen, A.: An

© Author(s) 2016. CC-BY 3.0 License.

755 improved parameterization for sulfuric acid-water nucleation rates for tropospheric and stratospheric conditions,
756 J. Geophys. Res., 107, 4622, doi:10.1029/2002JD002184, 2002.
757
758 Visschedijk, A. J. H., Zandveld, P., and Denier van der Gon, H. A. C.: TNO Report 2007 A R0233/B: A high
759 resolution gridded European emission database for the EU integrated project GEMS, Netherlands, Organization
760 for Applied Scientific Research, 2007.
761
762 Westervelt, D. M., Pierce, J. R., and Adams, P. J.: Analysis of feedbacks between nucleation rate, survival
763 probability and cloud condensation nuclei formation, Atmos. Chem. Phys., 14, 5577-5597, doi:10.5194/acp-14-
764 5577-2014, 2014.
765
766 Yu, F.: Effect of ammonia on new particle formation: A kinetic H_2SO_4-H_2O-NH_3 nucleation model constrained by
767 laboratory measurements, J. Geophys. Res., 111, D01204, doi:10.1029/2005JD005968, 2006a.
768
769 Yu, F., and Luo, G.: Simulation of particle size distribution with a global aerosol model: contribution of nucleation
770 to aerosol and CCN number concentrations, Atmos. Chem. Phys., 9, 7691– 7710, doi:10.5194/acp-9-7691-2009,
771 2009.
772
773 Yu, F., Luo, G., Bates, T. S., Anderson, B., Clarke, A., Kapustin, V., Yantosca, R. M., Wang, Y., and WU, S.:
774 Spatial distributions of particle number concentrations in the global troposphere: Simulations, observations, and
775 implications for nucleation mechanisms, J. Geophys. Res., 115, D17205, doi:10.1029/2009JD013473, 2010.
776
777 Zhang, Y., P. H. McMurry, F. Yu, and M. Z. Jacobson: A comparative study of nucleation parameterizations: 1.
778 Examination and evaluation of the formulations, J. Geophys. Res., 115, D20212, doi:10.1029/2010JD014150,
779 2010.
780
781
782
783
784

Geosci. Model Dev. Discuss., doi:10.5194/gmd-2016-21, 2016
Manuscript under review for journal Geosci. Model Dev.
Published: 11 February 2016
© Author(s) 2016. CC-BY 3.0 License.

Geoscientific Model Development Discussions
Open Access
EGU

785

786

787 Figures and figure captions

788 Table 1. Summary of PMCAMx-UF model simulations reported in this study. The arithmetic mean of
789 ground-level number concentration during May 2008 for particles larger than 0.8 nm (N_{tot}), 50 nm (N_{50})
790 and 100 nm (N_{100}) is given for each simulation. DE = default emissions, NE = new emissions. The
791 "default emissions" refer to the emissions used in Fountoukis et al., 2012 (simulation Napari-RADM-
792 DE).

Simulation name	NPF scheme	Cloud adjustment scheme	Emissions	Domain mean number concentration (cm^{-3})		
				N_{tot}	N_{50}	N_{100}
ACDC-TUV-DE	ACDC-based	TUV	Default	59200	1300	360
ACDC-RADM-DE	ACDC-based	RADM	Default	62000	1200	340
ACDC-TUV-NE	ACDC-based	TUV	Updated	48300	1300	380
Napari-TUV-DE	Scaled Napari et al., 2002	TUV	Default	8100	1500	410
Napari-RADM-DE	Scaled Napari et al., 2002	RADM	Default	9000	1500	400

793

794

Geosci. Model Dev. Discuss., doi:10.5194/gmd-2016-21, 2016
Manuscript under review for journal Geosci. Model Dev.
Published: 11 February 2016
© Author(s) 2016. CC-BY 3.0 License.

Geoscientific Model Development Discussions
Open Access
EGU

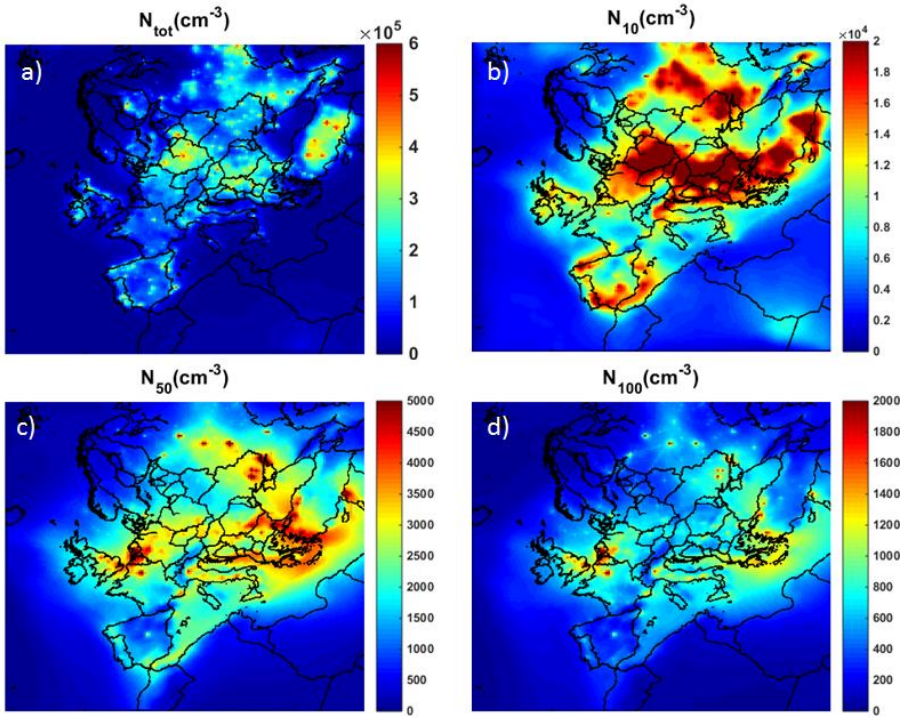

Figure 1. The simulated spatial distribution of the arithmetic mean of ground-level number concentration during May 2008 for particles larger than (a) 0.8 nm (N_{tot}), (b) 10 nm (N_{10}), (c) 50 nm (N_{50}), and (d) 100 nm (N_{100}). The PMCAMx-UF baseline simulation ACDC-TUV-DE is used (see Table 1). Note that different color bar scales are used for the different size ranges for readability.

Geosci. Model Dev. Discuss., doi:10.5194/gmd-2016-21, 2016
Manuscript under review for journal Geosci. Model Dev.
Published: 11 February 2016
© Author(s) 2016. CC-BY 3.0 License.

Geoscientific Model Development Discussions
Open Access
EGU

801

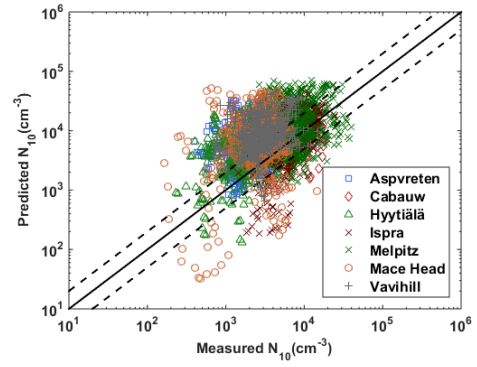

802

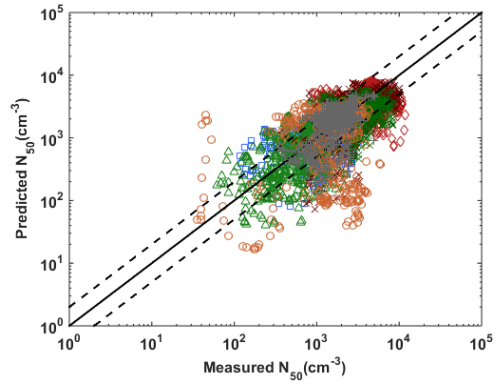

803

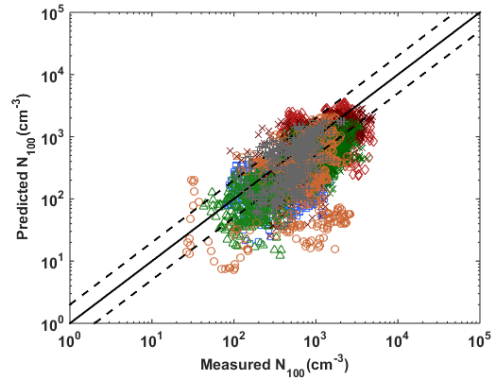

804 Figure 2. Comparison of predicted vs. measured hourly-averaged number concentration of
805 particles larger than 10 nm (N_{10}), 50 nm (N_{50}) and 100 nm (N_{100}) during May 2008 from the 7
806 EUSAAR measurement stations during the EUCAARI project. Lines corresponding to 1:1
807 (solid line), and 1:2 and 2:1 (dashed lines) are shown. The PMCAMx-UF model simulation ACDC-
808 RADM-DE is used (see Table 1).

809

810

Geosci. Model Dev. Discuss., doi:10.5194/gmd-2016-21, 2016
Manuscript under review for journal Geosci. Model Dev.
Published: 11 February 2016
© Author(s) 2016. CC-BY 3.0 License.

811

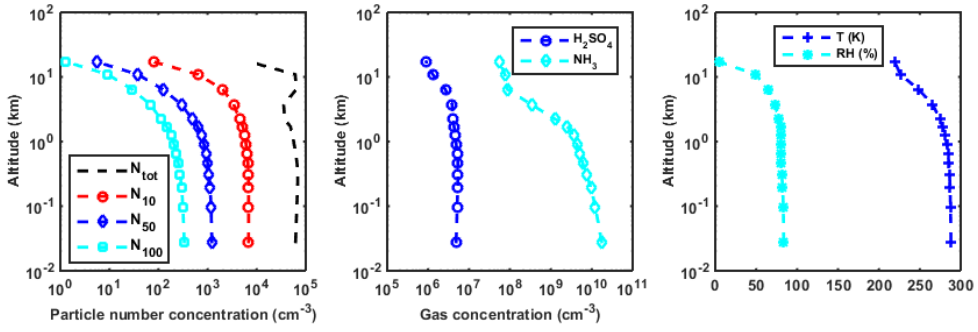

812

813 Figure 3. Vertical profiles of simulated variables averaged (arithmetic mean) over May 2008 and the
814 whole simulation domain. Left panel: number concentration (cm^{-3}) of particles larger than 0.8 nm (N_{tot}),
815 10 nm (N_{10}), 50 nm (N_{50}) and 100 nm (N_{100}). Middle panel: gas phase concentration (cm^{-3}) of sulfuric
816 acid (H_2SO_4) and ammonia (NH_3). Right panel: temperature (K) and relative humidity (%). The
817 PMCAMx-UF baseline simulation ACDC-TUV-DE is used (see Table 1).

818

Geosci. Model Dev. Discuss., doi:10.5194/gmd-2016-21, 2016
Manuscript under review for journal Geosci. Model Dev.
Published: 11 February 2016
© Author(s) 2016. CC-BY 3.0 License.

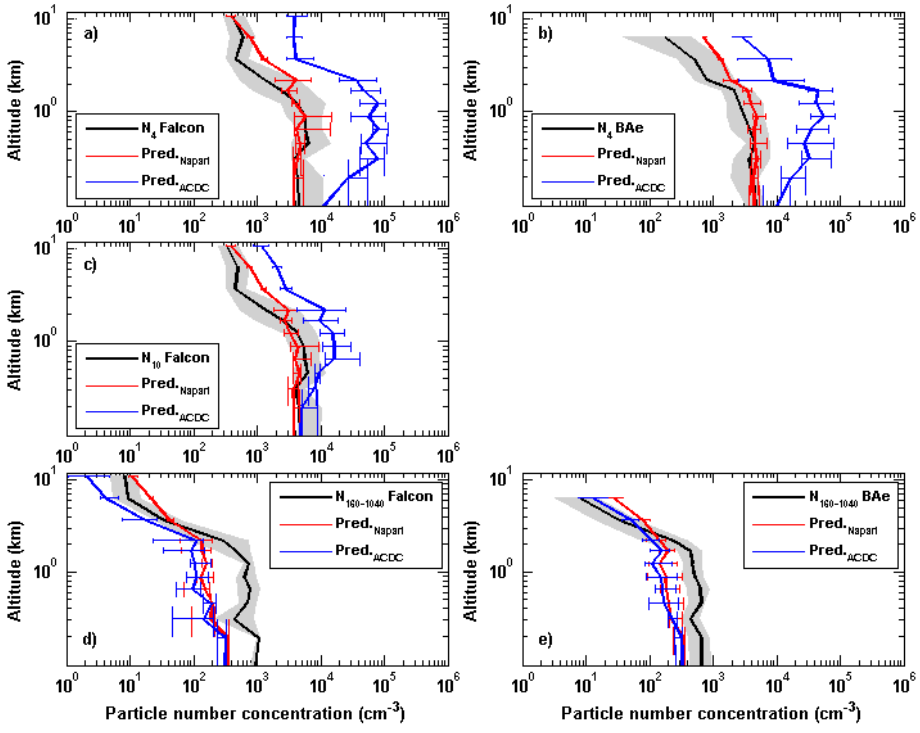

Figure 4. Vertical profiles of measured (black) and predicted (red and blue) particle number concentrations for the size ranges: (a) and (b) Larger than 4 nm (N_4) measurements collected by Falcon and BAe 146, respectively, (c) larger than 10 nm (N_{10}) measurements collected by Falcon 20, (d) and (e) 160-1040 nm ($N_{160\text{-}1040}$) measurements collected by Falcon and BAe 146, respectively, during May 2008. Red and blue lines show the predicted particle number concentrations by the PMCAMx-UF model using ACDC-based formation rates (ACDC-TUV-DE) and scaled Napari new particle formation scheme (Napari-TUV-DE), respectively. The lines show the median values of data points within each model layer, and the error bars and grey shading indicate the values between 25-th and 75-th percentiles of the model results and observations, respectively. Concentrations are given at ambient temperature and pressure.

Geosci. Model Dev. Discuss., doi:10.5194/gmd-2016-21, 2016
Manuscript under review for journal Geosci. Model Dev.
Published: 11 February 2016
© Author(s) 2016. CC-BY 3.0 License.

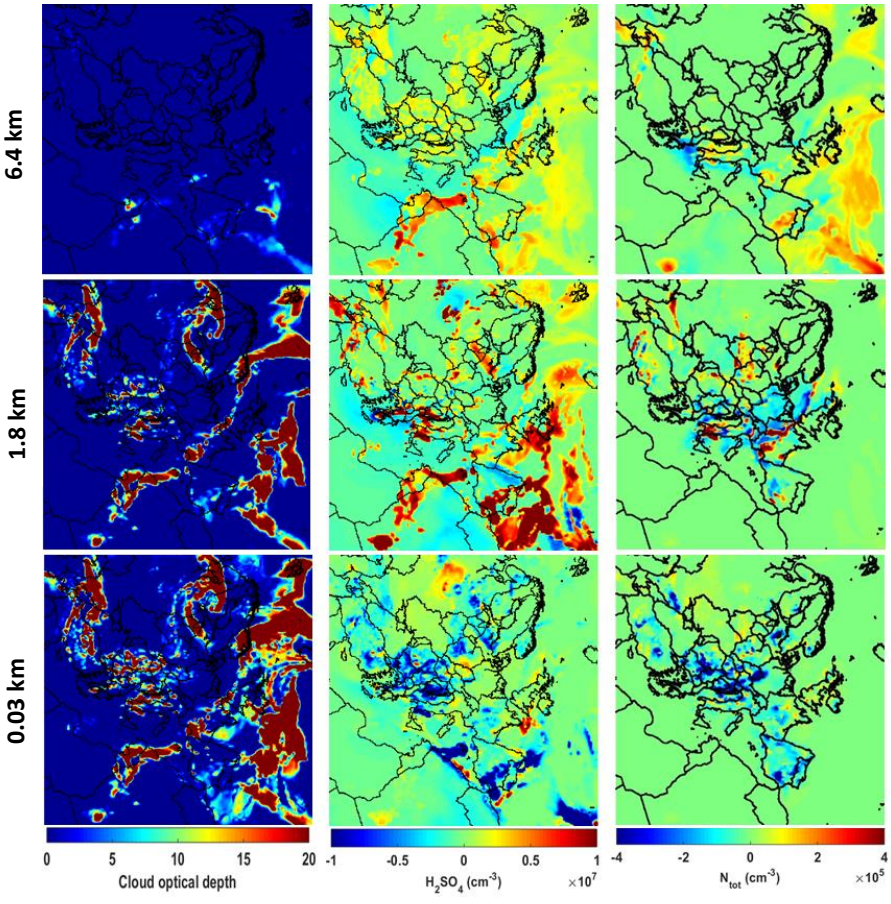

Figure 5. Left column: the total cloud optical depth supplied by WRF meteorology model. Middle column: the absolute difference between the predictions using the TUV (the simulation ACDC-TUV-DE; see table 1) and RADM (the simulation ACDC-RADM-DE) radiative transfer schemes within PMCAMx-UF for H_2SO_4 concentration. Right column: absolute difference between prediction using TUV and RADM schemes for total particle number concentrations N_{tot}. The parameters shown in the figure are snapshots on May 5, 2008 12:00 UTC at model layers 1 (mid-point altitude 0.03 km), 9 (mid-point altitude 1.7 km) and 12 (mid-point altitude 6.4 km).